

Antioxidant Activity of Ferulic Acid Alkyl Esters in a Heterophasic System: A Mechanistic Insight

CECILIA ANSELMI,^{*,†,‡} MARISANNA CENTINI,^{†,‡} PAOLA GRANATA,[§]
 ALESSANDRO SEGA,^{†,‡} ANNA BUONOCORE,^{†,‡} ANDREA BERNINI,[#] AND
 ROBERTO MAFFEI FACINO[§]

Dipartimento Farmaco Chimico Tecnologico, Università di Siena, Via Aldo Moro, 53100 Siena, Italy; Scuola di Specializzazione in Scienza e Tecnologia Cosmetiche, Facoltà di Farmacia, Università di Siena, Via della Diana 2, 53100 Siena, Italy; Istituto di Chimica Farmaceutica e Tossicologica, Facoltà di Farmacia, Università di Milano, Viale Abruzzi 42, 20131 Milano, Italy; and Dipartimento di Biologia Molecolare, Università di Siena, Via Fiorentina, 53100 Siena, Italy

The antioxidant activity of some esters of ferulic acid with the linear fatty alcohols C₇, C₈ (branched and linear), C₉, C₁₁, C₁₂, C₁₃, C₁₅, C₁₆, and C₁₈ has been studied in homogeneous and heterogeneous phases. Whereas in homogeneous phase all of the alkyl ferulates possessed similar radical-scavenging abilities, in rat liver microsomes they showed striking differences, the more effective being C₁₂ (**7**) (IC₅₀ = 11.03 μM), linear C₈ (**3**) (IC₅₀ = 12.40 μM), C₁₃ (**8**) (IC₅₀ = 18.60 μM), and C₉ (**5**) (IC₅₀ = 19.74 μM), followed by C₇ (**2**), C₁₅ (**9**), C₁₁ (**6**), branched C₈ (**4**), C₁₆ (**10**), and C₁₈ (**11**) (ferulic acid was the less active, IC₅₀ = 243.84 μM). All of the molecules showed similar partition coefficients in an octanol-buffer system. Three-dimensional studies (NMR in solution, modeling in vacuo) indicate that this behavior might be due to a different anchorage of the molecules with the ester side chain to the microsomal phospholipid bilayer and to a consequent different orientation/positioning of the scavenging phenoxy group outside the membrane surface against the flux of oxy radicals.

KEYWORDS: Alkyl ferulates; antioxidant/radical scavenging activity; acellular and cellular models; conformational analysis; intervention in biological membranes

INTRODUCTION

Ferulic acid alkyl esters have recently emerged as naturally occurring or synthetic agents with high promising biological properties due to their antioxidant and radical scavenging activities.

Such compounds are currently under investigation as potential leads for the prevention of free radical induced diseases in man, such as inflammation, cancer, atherosclerosis, and premature skin aging, all caused by an imbalance of tissue antioxidant status (*1*).

In particular, because of their suppressive activity on COX-2 gene expression, they have been recently claimed as cancer chemopreventive agents (*2*) etc. and are currently under pre-clinical evaluation.

In light of the possible development of new products for human health and, in addition, their potential application in the cosmetic field as UV filters and antioxidant/radical scavenging

agents, it is of paramount importance to understand the physicochemical parameters that govern their antioxidant activity, that is, alkyl chain length, hydrophobic properties, affinity of the molecule for the lipid substrate, and structure requirements for anchoring to the phospholipid bilayer.

Surprisingly, until now the mechanism(s) dictating the antioxidant potency of this important class of new molecules has (have) been rather neglected and limited to the following: (a) an observation of the overall lipophilic character of the molecule, that is, the partition coefficient in octanol/buffer (*3*); (b) an evaluation of the scavenging effect on the 1,1-diphenyl-2-picrylhydrazyl (DPPH) radical, the most general index of antioxidant activity; (c) an estimate of their protective effect against artificially induced free radicals in artificial membrane models (phosphatidylcholine liposomes, PC liposomes); and (d) an affinity factor calculated in membrane models (PC liposomes).

No detailed studies have ever been done on their protective effect working with cellular models that make use of physiological membranes or physiological free radical promoters, but above all using molecular descriptors that can give a deeper insight into the interaction with phospholipid membranes, such as three-dimensional structure and conformational properties.

* Address correspondence to this author at the Scuola di Specializzazione in Scienza e Tecnologia Cosmetiche, Via della Diana 2, 53100 Siena, Italy (telephone +39 577 232039; fax +39 577 232070; e-mail anselmic@unisi.it).

† Dipartimento Farmaco Chimico Tecnologico, Università di Siena.

‡ Scuola di Specializzazione in Scienza e Tecnologia Cosmetiche, Università di Siena.

§ Università di Milano.

Dipartimento di Biologia Molecolare, Università di Siena.

This represents the aim of the present study in which we have investigated the antioxidant properties of a series of *n*-alkyl ferulates of natural source or originating from chemical modification of naturally occurring compounds. The research was carried out using as membrane model rat liver microsomes, as free radical promoter the physiological couple Fe³⁺/ascorbic acid, and as physicochemical tool the conformational analysis using nuclear Overhauser effect spectroscopy (NOE).

This study was performed in an attempt to define (1) an optimum chain length of the molecules for anchoring to membrane binding sites, (2) orientation of the phenoxy group with respect to the membrane bilayer, and (3) whether the orientation/positioning on the membrane is affected by side-chain folding.

The results of the present study are evidence that three-dimensional arrangements with respect to the membrane bilayer play a key role in dictating the antioxidant ability of *n*-alkyl ferulates and furnish a reasonable explanation of the mechanism of their antioxidant intervention in biological membranes.

In addition, the findings here reported are the first to our knowledge that shed light on the three-dimensional behavior of these molecules and provide useful information for the design/bioavailability of new chemical antioxidant entities with photo-protective/radical scavenging properties.

MATERIALS AND METHODS

Instruments. Spectrophotometric studies were carried out in a computer-aided Perkin-Elmer Lambda 16 spectrophotometer (Perkin-Elmer, Monza, Italy). NMR analysis was performed on a 200 MHz Bruker AC-200 (Bruker Biospin, Milan, Italy).

The conformational study was carried out in vacuo using the AMBER force field and AMBER software (4). The oxygen radical absorbance capacity (ORAC) studies were carried out with a multiwell reader Victor² (Perkin-Elmer Life Sciences, Milan, Italy).

Materials. All of the organic solvents used were of analytical grade (Aldrich, Milan, Italy). Ferulic acid was supplied by Tsuno Rice Fine Chemicals, Wakayama, Japan.

1-Heptanol, 1-octanol, 2-ethyl-1-hexanol, 1-nonanol, 1-undecanol, 1-dodecanol, 1-tridecanol, 1-pentadecanol, 1-hexadecanol, 1-octadecanol, *p*-toluenesulfonic acid, DPPH, ferric chloride, adenosine 5'-diphosphate (ADP), ascorbic acid, and thiobarbituric acid (TBA) reagent were purchased from Aldrich. ORAC reagents, that is, 2,2'-azobis(2-aminopropane) dihydrochloride (AAPH) and R-phycoerythrin (R-PE) were purchased from Molecular Probes (Rome, Italy). Trdox (6-hydroxy-2,5,7,8-tetramethylchroman-2-carboxylic acid) was purchased from Sigma-Aldrich (Milan, Italy).

Isolation of Microsomes. Male Wistar rats (Charles River, Calco, LC, Italy; 220 ± 10 g body weight) were maintained in compliance with the policy on animal care expressed in the National Research Council guidelines (NRC 1985). Rat liver microsomes were isolated from the liver as previously described (5).

Animals were killed by decapitation, and livers were quickly removed and washed with isolation medium (ice-cold 0.25 M sucrose containing 10 mM Tris-HCl, pH 7.4). A 10% liver homogenate was made in isolation medium. Microsomes were isolated by differential centrifugation, washed twice with 10 mM phosphate buffer (pH 7.4), and suspended in the same buffer. All operations were carried out at 0–4 °C. The protein was estimated according to the Lowry method (6). In the lipid peroxidation experiments microsomes were diluted with 10 mM phosphate buffer (pH 7.4) (2.0 mg of protein/mL).

DPPH Assay. Methanol solutions (0.1 mL) of each compound (final concentrations = 5.0, 15.0, 25.0, and 50.0 μM) were added to 3.9 mL of 60 μM methanol DPPH solution (final volume = 4 mL), and the loss in absorbance at 517 nm was read after 90 min of incubation of the mixtures at room temperature in the dark (IC₅₀ value) and at 0 min, 1 min, and every 15 min until the reaction reached a plateau to calculate the antiradical power (ARP; = 1/EC₅₀). The antiradical activity was defined as the amount of antioxidant necessary to decrease the

initial DPPH concentration by 50% (efficient concentration = EC₅₀ - ((mol/L) antioxidant/(mol/L) DPPH) and as IC₅₀ (the concentration (μM) that leads to a 50% decrease in the original absorbance. DPPH solution in methanol served as the control. Special care was taken to minimize the loss of free radical activity of DPPH stock solution as recommended by Blois (7).

ORAC Assay (ORAC_{ROO}). The antioxidant activity was determined by using the ORAC assay, which evaluates the scavenging activity of the tested compounds against peroxy radicals, generated from the thermal decomposition of the radical initiator AAPH.

R-PE (16.7 nM in 75 mM phosphate saline buffer (pH 7)) was used as a target of free radical attack.

Trolox (5 μg/mL; 20 μM) was used as a control standard and prepared fresh daily. All fluorescence measurements were carried out on a plate reader maintained at 37 °C. The excitation filter was set at 485 nm and the emission filter at 530 nm.

The analyzer was programmed to record the fluorescence of R-PE every 5 min, for 2 h, after AAPH addition (3 mg/mL).

All compounds, including Trolox, were dissolved in DMSO (<0.1%) and then diluted in the mixture containing R-PE. DMSO was used to prepare blanks contained all of the reagents except the inhibitors.

Final results were calculated using the differences of area under the R-PE decay curves between blank and sample expressed as Trolox equivalents (μM).

Thiobarbituric Acid Assay. An aliquot of microsomal suspension was incubated for 15 min at 37 °C with test compounds at different concentrations (5–50 μM).

Then the reaction mixture was incubated for 1 h with 150 μM ferric chloride, 3 mM ADP, and 100 μM of ascorbic acid.

The extent of lipid peroxidation was assessed by measuring the content of malondialdehyde (MDA) in the incubation mixture according to the TBA assay (8).

In brief, the reaction mixture was treated with 1 mL of TBA reagent consisting of 0.37% TBA and 15% of trichloroacetic acid (TCA) in 0.5 N HCl and placed in a boiling water bath for 15 min, cooled, and centrifuged at 4000 rpm for 10 min; the supernatants were read at 532 nm, converting to nanomoles of MDA with an absorption coefficient of 156 mM⁻¹ cm⁻¹. Blanks were the overall reaction mixtures without TBA. Mean values of five determinations were used for the calculation.

Partition Coefficient in Octanol/PBS. A solution (200 μM) of the test compound in *n*-octanol was kept at 40 °C for 1 h, and the absorbance value at 254 was measured (A₀). An equal volume of PBS (pH 7.4) was added to the organic solution, and the mixture was stirred using a vortex mixer for 1 min and allowed to sit at 40 °C for 1 h.

After the mixture was centrifuged at 1000 rpm for 10 min, the absorbance at 254 nm of the organic layer was measured (A_i). The partition coefficient was expressed as A_i/A₀. A solution of *n*-octanol saturated with water was used as a blank.

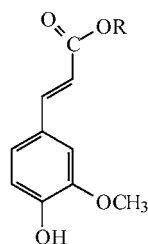
Conformational Analysis. NMR Analysis. ¹H NMR spectra were recorded in CDCl₃. Chemical shifts (δ) are indicated in parts per million with reference to tetramethylsilane, used as internal standard. Coupling constants (*J*) are reported in hertz. 2D-NOE (NOESY) spectra were recorded for 0.01 M solution in CDCl₃ with standard sequences.

Molecular Modeling. The conformational study was carried out in vacuo using the AMBER force field and AMBER software (4) and a new generation of the AMBER force field (9) suitable and modified for the compounds of the present study. Structures were built from scratch, and proton–proton distance restraints were calculated according to the observed NOE's strength: distance values of 3.0, 4.0, and 5.0 Å were used for strong, intermediate, and weak NOEs, respectively. A constant-temperature dynamics run with periodic temperature jumps (10) followed, according to the following protocol: 8 ps MD at 300 K, temperature jumps at 600 K for 4 ps to provide enough energy to pass conformational barriers, four repetitions of this cycle. A 75 ps MD run at 300 K followed. The same protocol was applied to all molecules. The root-mean-square deviation (rmsd) reached a maximal plateau value of 1.5 Å among all dynamics.

Statistical Analyses. Data are shown as mean ± standard deviation (SD) from five independent experiments. The statistical significance

Table 1. Spectral Data of Ferulic Acid Derivatives

compound	¹ H NMR (200 MHz, CDCl ₃)
C ₁₃ (8)	0.86 (t, 3H, J(21–22) = 6.3, H-22); 1.25 (bp, 20H, H-12-H-21); 1.68 (m, 2H, H-11); 3.90 (s, 3H, OCH ₃); 4.17 (t, 2H, J(10–11) = 6.8, H-10); 6.27 (d, 1H, J(7–8) = 16.2, H-8); 6.89 (d, 1H, J(5–6) = 8.0, H-5); 7.02 (d, 1H, J(2–6) = 2.2, H-2); 7.07 (dd, 1H, J(2–6) = 2.2, J(5–6) = 8.0, H-6); 7.58 (d, 1H, J(7–8) = 16.2, H-7)
C ₁₅ (9)	0.86 (t, 3H, J(23–24) = 6.2, H-24); 1.24 (bp, 24H, H-12-H-24); 1.68 (m, 2H, H-11); 3.91 (s, 3H, OCH ₃); 4.17 (t, 2H, J(10–11) = 6.6, H-10); 6.27 (d, 1H, J(7–8) = 15.8, H-8); 6.89 (d, 1H, J(5–6) = 7.9, H-5); 7.03 (d, 1H, J(2–6) = 2.4, H-2); 7.07 (dd, 1H, J(2–6) = 2.4, J(5–6) = 7.9, H-6); 7.58 (d, 1H, J(7–8) = 15.8, H-7)
C ₁₈ (11)	0.86 (t, 3H, J(26–27) = 6.5, H-27); 1.24 (bp, 30H, H-12-H-26); 1.67 (m, 2H, H-11); 3.90 (s, 3H, OCH ₃); 4.17 (t, 2H, J(10–11) = 6.6, H-10); 6.26 (d, 1H, J(7–8) = 15.8, H-8); 6.89 (d, 1H, J(5–6) = 8.0, H-5); 7.02 (d, 1H, J(2–6) = 2.3, H-2); 7.07 (dd, 1H, J(2–6) = 2.3, J(5–6) = 8.0, H-6); 7.58 (d, 1H, J(7–8) = 15.8, H-7)



- 1: R = H
 2: R = heptyl
 3: R = octyl
 4: R = 2-ethyl-1-hexyl
 5: R = nonyl
 6: R = undecyl
 7: R = dodecyl
 8: R = tridecyl
 9: R = pentadecyl
 10: R = hexadecyl
 11: R = octadecyl

Figure 1. Structures of ferulic acid (1) and its derivatives (2–11).

of differences between compounds was assessed by Student's *t* test and considered to be significant when the *P* value was ≤ 0.05 .

RESULTS

Compounds 2–11 (Figure 1) were synthesized according to standard procedure by reaction of ferulic acid with the corresponding alcohol (11). The crude products were purified on a silica gel column and identified by TLC, UV, and NMR analyses (11–13).

Table 1 reports the spectral data relative to those compounds that, to our knowledge, have not been previously found in the literature.

DPPH Assay. As preliminary screening for the study of the scavenging ability of ferulic acid (1) and its derivatives (2–11), we tested their quenching activity against the DPPH radical.

The DPPH test is carried out in a homogeneous phase and is rather unspecific: it gives a rough index of the scavenging activity because it measures the H radical/electron-transferring ability of an antioxidant versus the stable free radical DPPH.

As reported in Table 2 all of the compounds showed similar degrees of DPPH scavenging with IC₅₀ values ranging from 22 to 26 μ M and antiradical powers (ARP) (ARP = 1/EC₅₀) ranging from 2.2 to 2.83. No statistically significant differences among compounds were observed.

ORAC Assay. This test is also done in a homogeneous solution. It is more specific than the DPPH assay because measures the quenching ability against peroxy radicals generated from the thermal decomposition of the radical initiator (AAPH): it gives an index of the protective effect of each compound against peroxy radicals, which have as target the

Table 2. Scavenging Activity of Antioxidants of DPPH Radical

compound	IC ₅₀ ^a (μ M)	ARP ^b
ferulic acid (1)	21.98 \pm 2.13	2.78
C ₇ (2)	22.66 \pm 1.57	2.61
linear C ₈ (3)	22.94 \pm 1.38	2.60
branched C ₈ (4)	25.53 \pm 1.68	2.35
C ₉ (5)	24.64 \pm 1.89	2.45
C ₁₁ (6)	21.33 \pm 2.82	2.83
C ₁₂ (7)	26.62 \pm 2.57	2.20
C ₁₃ (8)	25.60 \pm 1.25	2.34
C ₁₅ (9)	24.93 \pm 1.63	2.57
C ₁₆ (10)	25.47 \pm 1.35	2.37
C ₁₈ (11)	24.97 \pm 1.95	2.38

^a Values are means \pm SD of five determinations. ^b Antiradical power.

Table 3. Protective Effect of Antioxidants Expressed in Trolox Equivalents

compound	Trolox equivalents ^a (μ M)
ferulic acid (1)	31.10 \pm 2.15
C ₇ (2)	28.60 \pm 1.62
linear C ₈ (3)	29.99 \pm 2.19
branched C ₈ (4)	28.85 \pm 1.80
C ₉ (5)	28.46 \pm 2.22
C ₁₁ (6)	28.31 \pm 1.88
C ₁₂ (7)	26.99 \pm 1.95
C ₁₃ (8)	28.57 \pm 3.13
C ₁₅ (9)	28.80 \pm 2.73
C ₁₆ (10)	28.46 \pm 0.68
C ₁₈ (11)	30.67 \pm 1.14

^a Values are means \pm SD of five determinations.

phycoerythrin protein. Protection is expressed in Trolox (the hydrophilic analogue of vitamin E) equivalents.

Also in this test the compounds showed similar degrees of activity (Table 3) ranging from 26 to 31 μ M (Trolox equivalents) and were not significantly different.

TBA Assay. The method is based on evaluation of the lipid peroxidation in microsomal membranes from rat liver. Microsomes are a physiological source of phospholipids with high polyunsaturated fatty acids contents. The TBARS test, although sometimes criticized when used for ex vivo experiments, appears to be the best, even if it is an *unspecific* indicator of the extent of lipid peroxidation in vitro. The results demonstrate that the efficacy of the compounds against Fe³⁺/ascorbic acid induced lipid peroxidation is dose-dependent. The concentrations able to inhibit 50% of the lipid peroxidation process for each derivative are reported in Figure 2.

We can appreciate a strong difference in antioxidant potency among the compounds. Linear C₈ (3) and C₁₂ (7) derivatives are the more active followed by C₁₃ (8), C₉ (5), C₇ (2), C₁₅ (9), C₁₁ (6), etc.; ferulic acid is the less active compound.

The greatest antioxidant potency of C₁₂ (7) in this model confirms previous findings in rat erythrocytes where the free

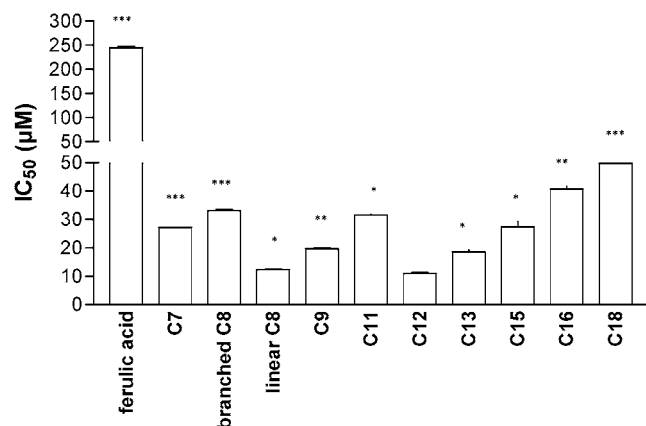


Figure 2. Antioxidant activity of the ferulic acid and its derivatives against lipid peroxidation. Values are means \pm SD of five determinations. Statistical analysis was done by Student's *t* test. Statistically different: *, $P < 0.05$; **, $P < 0.01$; ***, $P < 0.001$, versus C12.

radical promoter was the lipophilic organic hydroperoxide CuOOH. Also in this model C₁₂ (7) exhibited the highest radical scavenging activity because it showed maximal degree of membrane protection against the intracellular generated free radical stress.

Conformational Analysis. *NMR and Molecular Modeling Analyses.* NOESY experiments have been recorded for each compound in solution (0.01 M CDCl₃). Homonuclear 2D NOE effects between protons have been studied to investigate the possible main mean conformation of the alkyl chains. The complete NOE analysis for each ferulic acid derivative is reported in **Tables 4** and **5**. The main mean conformations of ferulic acid derivatives are shown in **Figure 3** (odd members, C₇ (2), C₉ (5), C₁₁ (6), C₁₃ (8), and C₁₅ (9); even members, linear C₈ (3), branched C₈ (4), C₁₂ (7), C₁₆ (10), and C₁₈ (11)).

These conformations were drawn on the basis of NOE results and subsequent computer molecular modeling analysis.

The most effective antioxidants, linear C₈ (3) and C₁₂ (7), are characterized by main mean folded conformations, by folding of the *n*-alkyl chain toward the ethylenic protons H7 (anticlockwise) or H8 (clockwise), and by a strong NOE between H8 and H3, suggesting that ethylenic and aromatic moieties are close to coplanarity. In light of these features C₁₆ (10) should also be one of the most effective antioxidants, possessing all of the characteristics listed above. Indeed, C₁₆ (10) is one of the less active compounds. This experimental fact puts forward another feature not previously considered: the chain length. It seems that linear C₈ (3) and C₁₂ (7) have the optimum chain length for efficient (for antioxidant activity) clockwise and anticlockwise folding, respectively.

The NOE analysis along the series of ferulic acid esters, C₇–C₁₈ (2–11), should give more insight on the conformational parameters connected with antioxidant activity. The C₇ (2) derivative has main mean folded conformations (clockwise), but the folding of the alkyl chain is toward the methoxy group as indicated by the NOE (OCH₃ \leftrightarrow H15) and there is no NOE between H8 and H3 (aromatic and ethylene planes are far from coplanarity). In C₉ (5) the folding of the alkyl chain is toward the ethylenic proton H7, but the NOE involved is weak (H7 \leftrightarrow H17) and there is no NOE between H8 and H3. On the other hand, in branched C₈ (4) folding is absent, but there is a strong NOE between H8 and H3. The C₁₁ (6) derivative presents conformations with folding toward the ethylenic moiety, but they have little weight because the NOE involved (H8 \leftrightarrow H19) is weak; no NOE is present between H8 and H3. Folded

conformations have more weight in the description of the main mean conformation of C₁₃ (8) than they have for C₁₁ (6). However, in C₁₃ (8) the alkyl chain folds on itself as indicated by the NOE (H9 \leftrightarrow H21). A NOE is present between protons H8 and H3. Passing to C₁₅ (9) we can note on the basis of NOE results that folded conformations are important in this compound, but as in C₁₃ (8) the folding of the alkyl chain is on itself (H9 \leftrightarrow H23). No NOE is present between H8 and H3. In the last derivative studied, C₁₈ (11), folding of the alkyl chain is completely absent, and only a quite weak NOE could be detected between H8 and H3.

Thus, the NOE analysis clearly shows that folding of the alkyl chain toward the ethylenic moiety and an almost coplanar arrangement between ethylenic and aromatic planes are key conformational parameters for antioxidant activity in this series of compounds. This analysis offers a rationale for interpreting the results presented in **Figure 2**. Indeed, weakening of one or both of these features provokes a decreasing in antioxidant activity.

Besides the conformational parameters, there is also a key structural parameter to be taken into consideration: the chain length. Indeed, from C₁₆ (10) onward (but likely from C₁₃ (8) onward) the antioxidant activity decreases even if the conformational features are satisfied simply because the chain is too long.

DISCUSSION

The evaluation of the antioxidant activity with the DPPH test in terms of both ARP and IC₅₀ does not show significant differences among compounds.

The same is true for the ORAC assay, which gives a mean value of Trolox equivalents similar for all of the ferulates (i.e., 28–30 μ M, **Table 3**).

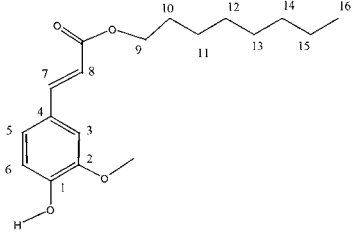
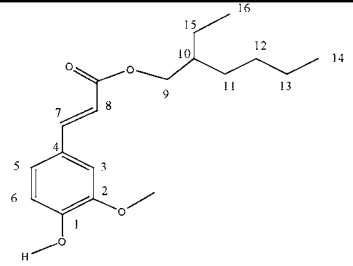
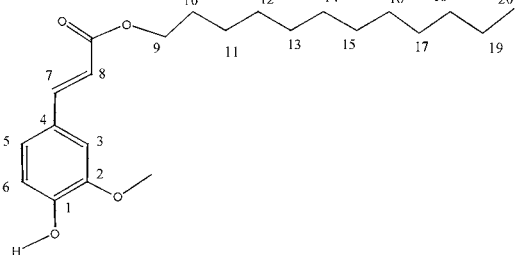
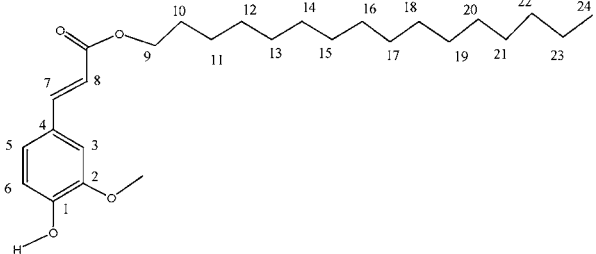
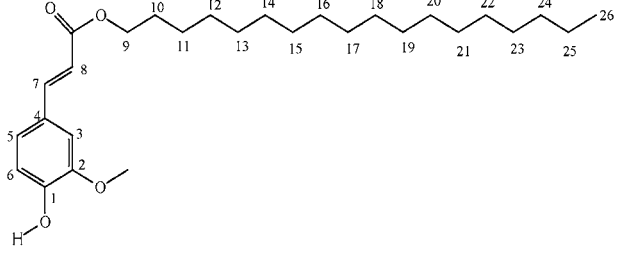
This means that, in a homogeneous solution, the modification of the side chain (lengthening/ramification) does not perturb, through intramolecular interactions, (between the side chain and the phenoxy nucleus), the antioxidant potency of the molecules. Examination of the lipophilic character of the molecules with the conventional approach—partition coefficient (octanol/PBS)—shows approximately the same degree of lipophilicity for all of the derivatives (\sim 0.970, **Table 6**).

Because these findings were difficult to reconcile with the differences in antioxidant potency observed in the heterogeneous phase, we became aware of the possibility that the latter may be dictated by a different anchorage of the side chain with membrane phospholipids.

Very likely different anchorages would affect in different ways the orientation/positioning of the radical scavenging nucleus (the phenoxy moiety), which must be constrained outside the bilayer surface to quench the flux of free oxy radicals generated by the physiological couple Fe³⁺/ascorbic acid.

The comparative analysis of the results from NMR (NOESY experiments) and subsequent computer modeling studies and of those relative to microsomal antilipoperoxidant activity gives strength to this assumption because it clearly shows that (1) the anchoring with the phospholipid membrane is favored when the side chain of the molecule has a high degree of conformational flexibility, that is, it is able to bend in a loop conformation toward the ethylenic moiety and or on itself, and (2) the anchoring is favored when the stability of this folded conformation is maximal: this happens when the side chain fits into an optimal length.

Table 4. Numbering System of Compounds **3**, **4**, **7**, **10**, and **11** (Even Members) Used throughout the Text and 2D-NOE (NOESY) Results

Ferulic acid derivative: <i>linear</i> C ₈ (3)	NOE effect	Strength
	OCH ₃ ↔ H ₉ H ₃ ↔ H ₈ H ₃ ↔ OCH ₃ H ₈ ↔ H ₁₆ H ₉ ↔ H ₁₆ OCH ₃ ↔ H ₁₆	Strong Strong Strong Medium/Strong Medium Medium
Ferulic acid derivative: <i>branched</i> C ₈ (4)	NOE effect	Strength
	OCH ₃ ↔ H ₉ H ₃ ↔ H ₈ OCH ₃ ↔ H ₃	Strong Strong Strong
Ferulic acid derivatives: C ₁₂ (7)	NOE effect	Strength
	OCH ₃ ↔ H ₃ H ₃ ↔ H ₈ H ₇ ↔ H ₂₀ H ₁₀ ↔ H ₂₀	Strong Strong Medium/Strong Medium/Strong
Ferulic acid derivative: C ₁₆ (10)	NOE effect	Strength
	OCH ₃ ↔ H ₃ H ₃ ↔ H ₈ H ₇ ↔ H ₂₄ H ₁₀ ↔ H ₂₄	Strong Strong Medium/Strong Medium/Strong
Ferulic acid derivative: C ₁₈ (11)	NOE effect	Strength
	OCH ₃ ↔ H ₃ H ₃ ↔ H ₈ OCH ₃ ↔ H ₉	Medium/Strong Medium/Strong Medium/Strong

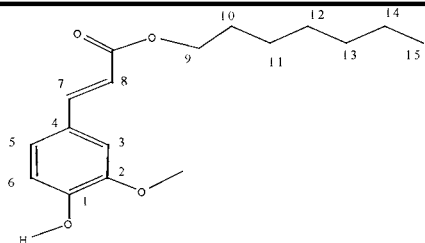
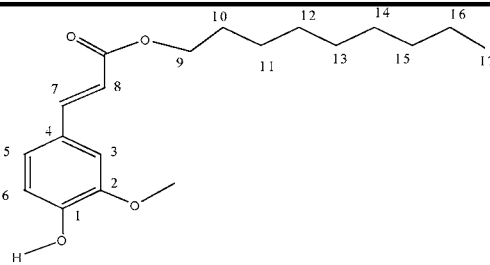
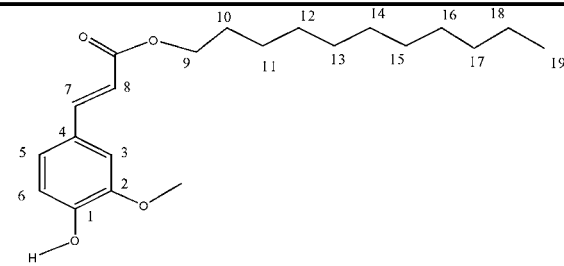
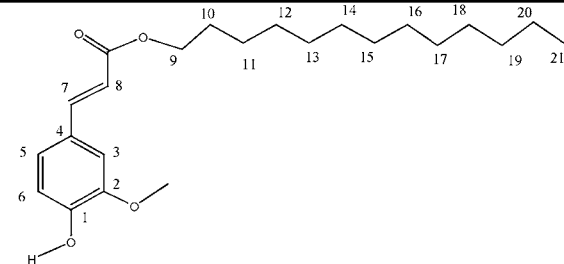
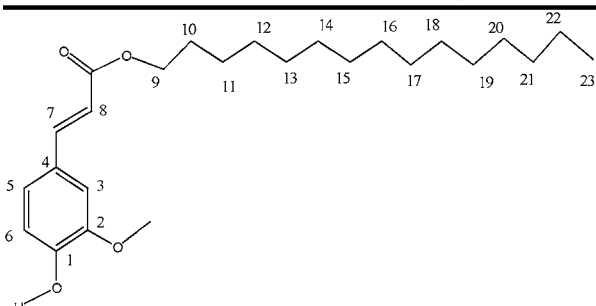
In fact, if we examine in detail the behavior of the compounds we find that in the C₇ derivative (**2**) (see the modest antioxidant activity, IC₅₀ = 27.54 μM) the side chain shows a weak bending but toward the O-methoxy residue (**Figure 3**).

In the C₉ derivative (**5**) this bending is more pronounced and involves interactions between the terminal methyl group and the ethylenic unit: this results in an increase of the antioxidant activity (IC₅₀ = 19.74 μM).

For C₁₁ (**6**) the bending is weak and, above all, the folded conformation shows a spatial arrangement (the presence of hindering groups, **Figure 3**) unfavorable for fitting inside the membrane (IC₅₀ = 31.61 μM).

In C₁₃ (**8**) the bending is weak but the folded conformation involves also the alkyl chain: this makes the molecule to reach a spatial arrangement more suited for penetrating inside the bilayer (IC₅₀ = 18.64 μM).

Table 5. Numbering System of Compounds **2**, **5**, **6**, **8**, and **9** (Odd Members) Used throughout the Text and 2D-NOE (NOESY) Results

Ferulic acid derivative: C ₇ (2)	NOE effect	Strength
	OCH ₃ ↔ H ₉ OCH ₃ ↔ H ₃ OCH ₃ ↔ H ₁₅	Medium/Strong Weak Medium
Ferulic acid derivative: C ₉ (5)	NOE effect	Strength
	OCH ₃ ↔ H ₉ OCH ₃ ↔ H ₃ H ₇ ↔ H ₁₇	Strong Very strong Weak
Ferulic acid derivatives: C ₁₁ (6)	NOE effect	Strength
	OCH ₃ ↔ H ₃ OCH ₃ ↔ H ₉ H ₉ ↔ H ₁₉ H ₈ ↔ H ₁₉	Medium Strong Weak Weak
Ferulic acid derivative: C ₁₃ (8)	NOE effect	Strength
	OCH ₃ ↔ H ₃ OCH ₃ ↔ H ₉ H ₉ ↔ H ₂₁ H ₈ ↔ H ₃	Medium Strong Medium/Weak Medium
Ferulic acid derivative: C ₁₅ (9)	NOE effect	Strength
	OCH ₃ ↔ H ₃ OCH ₃ ↔ H ₉ H ₉ ↔ H ₂₃	Strong Strong Strong

In C₁₅ (**9**) the bending of the side chain is weak and the increase in the length of the chain plays a negative role by hampering the binding.

Among the even members of the series (**Figure 3**), branched C₈ (**4**) bears the side chain in a straight form, and this hampers the interaction with the bilayer (IC₅₀ = 33.16). Conversely, linear C₈ (**3**) shows a strong interaction with the hydrogen of

the ethylenic group, which leads to a folded conformation. This results in a dramatic rise in antioxidant potency (IC₅₀ = 12.40 μM).

An analogous behavior is observed in C₁₂ (**7**), where this interaction is strong: in this case the possibility/stability of the loop conformation is maximal among the compounds because folding involves also the alkyl chain and optimal is the length

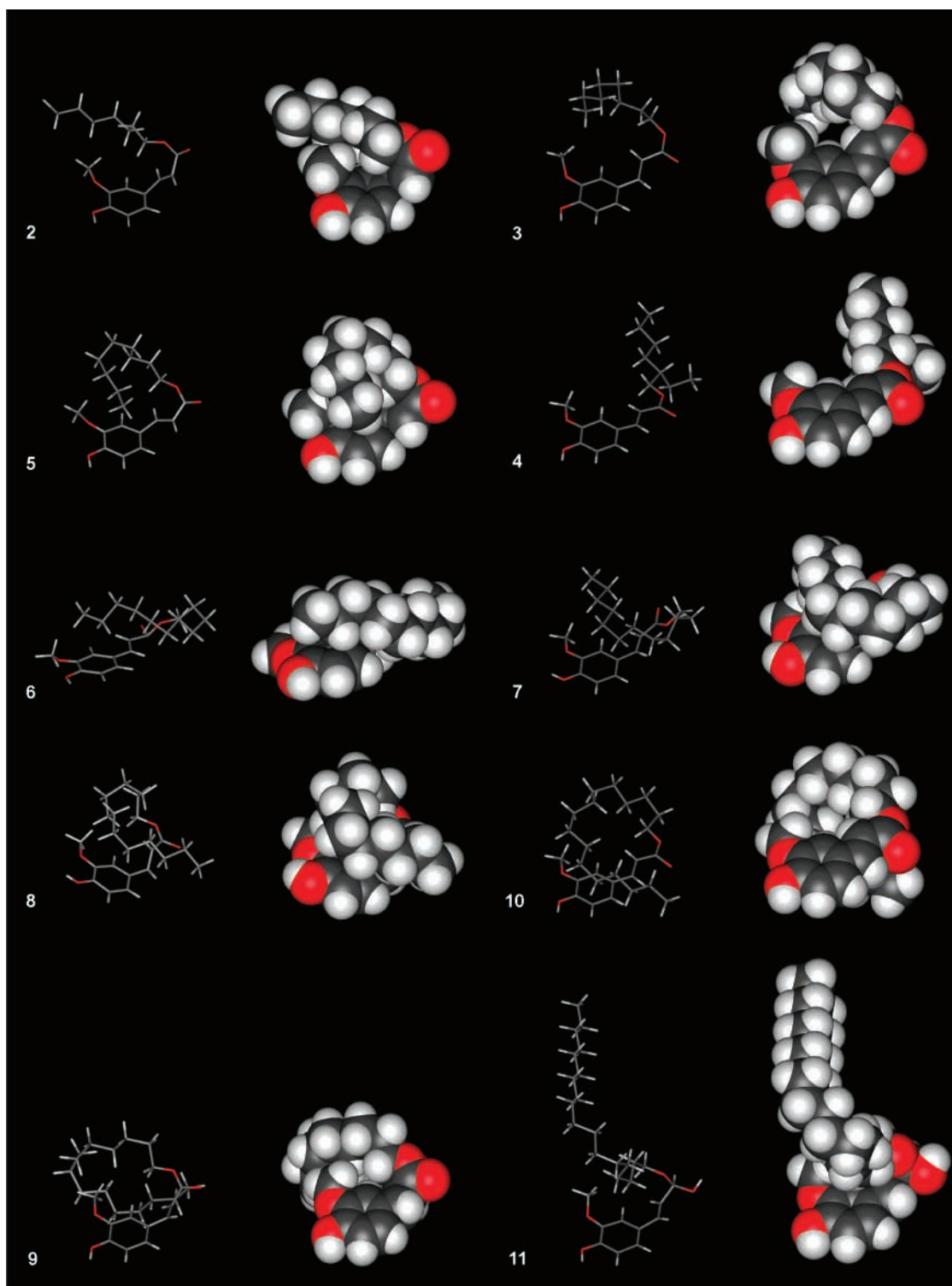


Figure 3. Most-probable conformations of ferulic acid derivatives in CDCl_3 solution as inferred from NMR experiments and molecular modeling. Odd members (C_7 (**2**), C_9 (**5**), C_{11} (**6**), C_{13} (**8**), and C_{15} (**9**)) are given on the left side and even members (linear C_8 (**3**), branched C_8 (**4**), C_{12} (**7**), C_{16} (**10**), and C_{18} (**11**)) on the right.

of the side chain (highest antioxidant activity of $\text{IC}_{50} = 11.03 \mu\text{M}$).

The behavior of the C_{16} derivative (**10**) is similar to that of linear C_8 (**3**) (the bending still involves the interaction with the hydrogen of the ethylenic group, and it is of medium strength), but the stability of the loop conformation is weak. This results in a loss of antioxidant potency ($\text{IC}_{50} = 40.79 \mu\text{M}$).

In the C_{18} derivative (**11**) there is no bending because there is no interaction between the side chain and the ethylenic

moiety: the spatial conformation of the side chain is in a straight form and the antioxidant potency is even lower ($\text{IC}_{50} = 49.78 \mu\text{M}$).

With regard to the type of bending, clockwise or anticlockwise, it is still under investigation whether it can play a significant role in side-chain anchoring.

In conclusion, the results of this study furnish a mechanistic explanation for the different antioxidant activities of alkyl ferulates in microsomal membranes and emphasize the impor-

Table 6. Partition Coefficients of Antioxidants in Octanol/Phosphate Saline Buffer (PBS)

compound	partition coefficient ^a
ferulic acid (1)	0.130 ± 0.010
C ₇ (2)	0.960 ± 0.020
linear C ₈ (3)	0.966 ± 0.015
branched C ₈ (4)	0.968 ± 0.013
C ₉ (5)	0.980 ± 0.015
C ₁₁ (6)	0.972 ± 0.017
C ₁₂ (7)	0.970 ± 0.011
C ₁₃ (8)	0.975 ± 0.011
C ₁₅ (9)	0.982 ± 0.018
C ₁₆ (10)	0.962 ± 0.019
C ₁₈ (11)	0.970 ± 0.012

^a Values are means ± SD of five determinations.

tance of this approach (study of three-dimensional arrangements) for the understanding of the biological activity of ferulates in cellular and more complex in vivo systems.

Finally, we can extrapolate from this study important information on the mechanism and strength of binding of these compounds with skin surface lipid and hence on their substantivity on the skin.

This is of paramount importance in the design/synthesis of new photoprotectant agents with UV filtering/antioxidant properties.

LITERATURE CITED

- (1) Murakami, A.; Nakamura, Y.; Koshimizu, K.; Takahashi, D.; Matsumoto, K.; Hagihara, K.; Taniguchi, H.; Nomura, E.; Hosoda, A.; Tsuno, T.; Maruta, Y.; Kim, H. W.; Kawabata, K.; Ohigashi, H. F15, a hydrophobic derivative of ferulic acid, suppresses inflammatory responses and skin tumor promotion: comparison with ferulic acid. *Cancer Lett.* **2002**, *180*, 121–129.
- (2) Hosoda, A.; Ozaki, Y.; Kashiwada, A.; Mutoh, M.; Wakabayashi, K.; Mizuno, K.; Nomura, E.; Taniguchi, H. Syntheses of ferulic acid derivatives and their suppressive effects on cyclooxygenase-2 promoter activity. *Bioorg. Med. Chem.* **2002**, *10*, 1189–1196.
- (3) Kikuzaki, H.; Hisamoto, M.; Hirose, K.; Akiyama, K.; Taniguchi, H. Antioxidant properties of ferulic acid and its related compounds. *J. Agric. Food Chem.* **2002**, *50*, 2161–2168.
- (4) Pearlman, D. A.; Case, D. A.; Caldwell, J. W.; Ross, W. S.; Cheatham III, T. E.; Ferguson, D. M.; Seibel, G. L.; Singh, U. C.; Weiner, P. K.; Kollman, P. A. AMBER 4.1, University of California, San Francisco, 1995.
- (5) Maffei Facino, R.; Carini, M.; Genchi, C.; Tofanetti, O.; Casciarri, I. Hydroxynimesulide, the main metabolite of nimesulide, prevents the hydroperoxide/hemoglobin-induced hemolysis of rat erythrocytes. *Pharmacol. Res.* **XXI** **1989**, *5*, 549–560.
- (6) Markwell, M. A.; Haas, S. M.; Tolbertr, N. E.; Bieber, L. L. Protein determination in membrane and lipoprotein samples: manual and automated procedures. *Methods Enzymol.* **1981**, *72*, 296–303.
- (7) Blois, M. Antioxidant determinations by the use of stable free radical. *Nature* **1958**, *181*, 1199–1200.
- (8) Casini, A. F.; Ferrali, M.; Pompella, A.; Maellaro, E.; Comporti, M. Lipid peroxidation and cellular damage in extrahepatic tissues of bromobenzene intoxicated mice. *Am. J. Pathos.* **1986**, *123*, 520–531.
- (9) Comell, W. D.; Cieplak, P.; Bayly, C. I.; Gould, I. R.; Merz, K. M.; Freguson, D. M.; Spellmeyer, D. C.; Fox, T.; Caldwell, J. W.; Kollman, P. A. A second generation force field for the simulation of proteins, nucleic acids, and organic molecules. *J. Am. Chem. Soc.* **1995**, *117*, 5179–5197.
- (10) Gharbi-Benarous, J.; Ladam, P.; Delaforge, M.; Girault, J. Conformational analysis of major metabolites of macrolide antibiotics roxithromycin and erythromycin A with different biological properties by NMR spectroscopy and molecular dynamics. *J. Chem. Soc., Perkin Trans. 2* **1993**, 2303–2321.
- (11) Taniguchi, H.; Nomura, E.; Tsuno, T.; Minami, S. Ferulic acid ester antioxidant/UV absorbent. Eur. Patent Appl. 0681 825 A2, 1998.
- (12) Bernards, M. A.; Lewis, N. G. Alkyl ferulates in wound potato tubers. *Phytochemistry* **1992**, *31*, 3409–3412.
- (13) Kawanishi, K.; Yasufuku, J.; Ishikawa, A.; Ashimoto, Y. Long-chain alkyl ferulates in three varieties of *Ipomoea batatas* (L.) Lam. *J. Agric. Food Chem.* **1990**, *38*, 105–108.

Received for review February 27, 2004. Revised manuscript received July 14, 2004. Accepted August 7, 2004. This work was financially supported by MIUR (Rome) as a Project within PRIN 2003. The financial support of Tsuno Rice Fine Chemicals is gratefully acknowledged.

JF049671X